Perovskite Phases

DOI: 10.1002/anie.201002301

Trends in Stability of Perovskite Oxides**

*Federico Calle-Vallejo, José I. Martínez, Juan M. García-Lastra, Mogens Mogensen, and Jan Rossmeisl**

Perovskite oxides with general formula AMO_3 have a large variety of applications as dielectrics and piezoelectrics,[1] ferroelectrics[2] and/or ferromagnetic materials,[3] among others. Rare earth and alkaline earth metal perovskites are useful as catalysts for hydrogen generation,[4] as oxidation catalysts for hydrocarbons,[5] and as effective and inexpensive electrocatalysts for state-of-the-art fuel cells,[6] mainly due to the possibility of tuning their mixed ionic–electronic conductivity through substitution of A and M and subsequent formation of oxygen vacancies. Despite the general interest in perovskites, so far there have been no ab initio studies devoted to their formation energies, and the trends in stability are unknown.

Among the available theoretical techniques to investigate perovskites, DFT is an appealing candidate, since it has proved useful for understanding metals and alloys at the atomic scale.[7] Nevertheless, the well-known shortcoming of DFT in describing strongly correlated systems has prevented its use for the estimation of properties such as band gaps and electron localization–delocalization of oxides, and there are numerous corrections.[8]

Despite these limitations, Figure 1a shows the experimental formation energies from elements and O_2 of 20 perovskites at 298 K and the corresponding standard DFT energies using the RPBE-GGA[9] exchange-correlation functional. The simulations are able to reproduce trends in the formation energies, and the calculated energies are shifted by about 0.75 eV compared to experiments. The A component is Y, La, Ca, Sr, or Ba, while M is a 3d metal from Ti to Cu. However, it is possible to combine the formation energies of these compounds with those of their sesquioxides (A_2O_3 and M_2O_3), rutile dioxides (MO_2), monoxides (AO and MO), and O_2 to reproduce the energetics of several reactions (Figure 1b–d). The reactions are shown in the Supporting Information. The excellent correspondence between experiments and theory shows that DFT very accurately captures the mixing energies between oxides. The chemical reaction depicted in Figure 1a and the way of representing its Gibbs energy, are given by Equations (1) and (2).

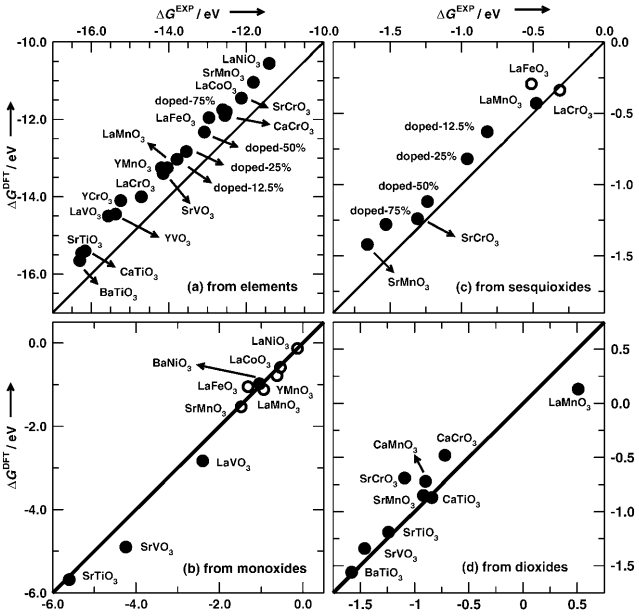

Figure 1. DFT calculated free energies of several reactions versus experimental values available in the literature, from a) A = Y, La, Ca, Sr, Ba and elements, b) A_2O_3/AO and monoxides, c) A_2O_3/AO and sesquioxides, and d) A_2O_3/AO and dioxides. As a guide to the eye, perfect agreement is marked by a line with $y = x$. The percentages of the doped perovskites represent the amount x of Sr in $La_{1-x}Sr_xMnO_3$. Reactions at 298 K are represented by filled circles, whereas empty circles denote reactions at 1273 K. References for the experiments are provided in the Supporting Information.

$$A + M + {}^3/_2O_2 \rightarrow AMO_3 \quad (1)$$

$$\Delta G^{form} = G_{AMO_3} - G_A - G_M - {}^3/_2G_{O_2} \quad (2)$$

In terms of trends the agreement is beyond the expected accuracy of DFT in general, but the shift is about 0.75 eV. We note that imitations in O_2 description by DFT are well known and some alternatives have been proposed, obtaining remarkable agreements with experiments.[8c,10] We obtain the total DFT energy of O_2 indirectly from the tabulated Gibbs energy of formation of water and from the DFT energies of H_2

[*] F. Calle-Vallejo, Dr. J. I. Martínez, Dr. J. M. García-Lastra, Prof. J. Rossmeisl
Center for Atomic-Scale Materials Design
Department of Physics, Technical University of Denmark
2800 Kgs. Lyngby (Denmark)
Fax: (+45) 4593-2399
E-mail: jross@fysik.dtu.dk
Prof. M. Mogensen
Fuel Cells and Solid State Chemistry Department
Risoe National Laboratory for Sustainable Energy, DTU
Frederiksborgvej 399, 4000 Roskilde (Denmark)

[**] CAMD is funded by the Lundbeck foundation. We acknowledge support by the Danish Council for Strategic Research via the SERC project, the DCSC, and the STREP-EU APOLLON-B project through grant nos. 2104-06-0011, HDW-1103-06, and NMP3-CT-2006-033228, respectively. We thank Prof. F. Flores and Prof. H. Yokokawa for their comments.

Supporting information for this article is available on the WWW under http://dx.doi.org/10.1002/anie.201002301.

and H_2O, which are accurately described using the exchange achieved by the RPBE-GGA functional.[8c,11] This reference has previously been used to obtain accurate formation energies of rutile oxides and has also been applied to calculate the adsorption energies of various oxides, including perovskites.[10,12] The reason of the shift is therefore not related to the reference state. We speculate that the localized nature of d electrons of the 3d metals in these perovskites is not well captured at this level of theory due to their self-interaction, giving rise to a large part of the constant shift in Figure 1 a. The rest of the shift comes from the deviations in the formation of the A oxides (A_2O_3 and/or AO). Nevertheless, the differences in formation energies between perovskites are very accurately accounted for by standard DFT, as shown in Figure 2. We remark that the use of another

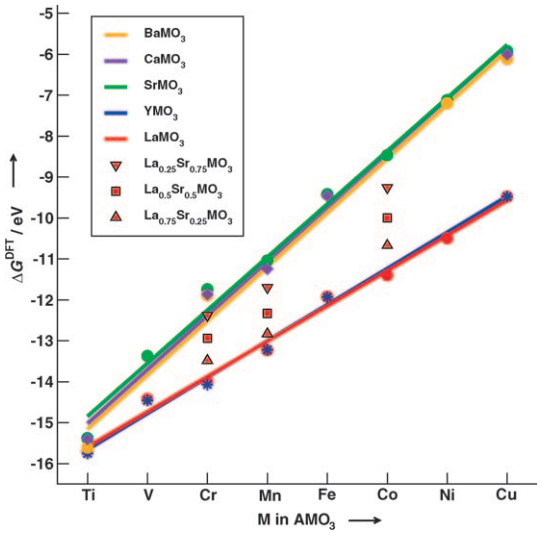

Figure 2. Trends in formation energies from elements for various families of perovskites (AMO_3), in terms of the atomic number of M. Symbols indicate calculated values for individual perovskites, and lines show the best fit for each family. Perovskites having the same oxidation state for A and M (+III, A = Y, La) are more stable than those in which they are different (+II and +IV, A = Ca, Sr, Ba), and their decay in stability is less pronounced. The positions of $La_{1-x}Sr_xMO_3$ perovskites, indicated by ▼, ■, ▲, support the idea that the effect is due to the oxidation states of the constituents. Note that stability with respect to the elements does not guarantee overall stability of the compounds.

exchange-correlation functional or a different value for O_2 would only shift the calculated stabilities by a constant number, while the qualitative trends and the relative differences would remain unchanged.

All families of perovskites exhibit a systematic linear scaling between their energetics and the atomic number of M. The scaling in Figure 2 was previously revealed by experiments only for some La perovskites at 1273 K.[13] We extend this behavior to other families of perovskites, and the insight allows the following generalization: the slope of the lines is determined by the oxidation states of A and M. Therefore, these compounds could be divided into two groups: perovskites with the same oxidation state for A and M (+III for $A'MO_3$; A′ = Y, La), and perovskites in which their oxidation states differ (+II and +IV for $A''MO_3$; A″ = Ca, Sr, and Ba). The former are more stable than the latter and their stabilities along the 3d series decrease more slowly, that is, their lines have less steep slopes. This could be attributed to the higher oxidation state forced onto M in $A''MO_3$ (a further discussion on this aspect is provided in the Supporting Information). The formation energies of perovskites in each group are approximately constant for materials with the same M constituent, independent of A. For example, the energetics of $SrCrO_3$ gives a good estimative of those of $CaCrO_3$ and $BaCrO_3$. Doped perovskites ($A'A''MO_3$) have intermediate formation energies between those of the pure counterparts, in accordance to the degree of doping. This behavior supports the idea that the difference between the groups is a matter of oxidation states. The use of simple parameters like the atomic numbers to estimate the formation energies of perovskites is easier and more intuitive than the common use of structural parameters such as the Goldschmidt factor or the Shannon's radii.[14]

Finally, let us explain the origin of the differences in stability of $A'MO_3$ by means of Figure 3. An expression similar to Equation (2) represents the formation energies of

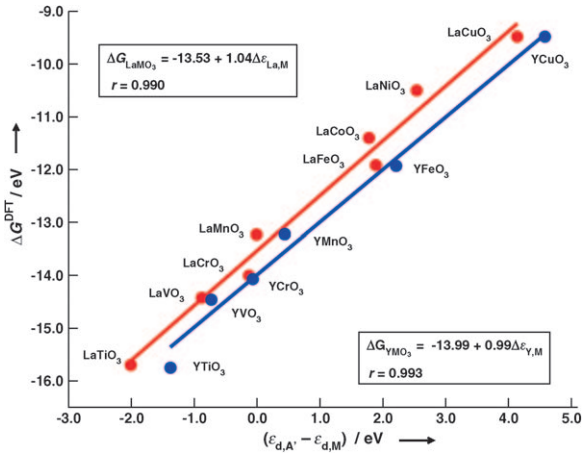

Figure 3. DFT-calculated free energies of formation of $LaMO_3$ (red) and YMO_3 (blue) versus the differences in d-band centers of La/Y and M. The intercept with the *y* axis is equivalent to the formation energy of the sesquioxides A'_2O_3 (A′ = Y, La) plus the deformation energy of these oxides from their most stable symmetries to space group *Pm*3*m*. Therefore, formation of these perovskites can be seen as destabilizations of the A'_2O_3 oxides by M/A′ swapping.

La_2O_3 and Y_2O_3 from the elements. By adding and subtracting $G_{A'}$ to and from Equation (2) and combining with the formation energy of the sesquioxides, one gets Equation (3).

$$\Delta G^{\mathrm{form}} = \Delta G_{A'_2O_3} - \left(G_M + G_{A'_2O_3} - G_{A'MO_3} - G_{A'}\right) \quad (3)$$

The term in parentheses in Equation (3) corresponds to a reaction step in which A′ in an A'_2O_3 lattice is replaced by M to form the perovskite structure. Thus, the reaction could be seen as the formation of A'_2O_3 followed by a lattice deformation and swapping between atoms resulting in

$A'MO_3$. The formation energy can then be expressed as Equation (4).

$$\Delta G^{\text{form}} = \Delta G_{A'_2O_3} + \Delta G_{\text{deformation}} + \Delta G_{\text{swap}} \quad (4)$$

The DFT formation energies of La_2O_3 and Y_2O_3 are -16.98 and -17.85 eV, respectively (-17.70[15] and -18.79 eV,[16] experimentally). The deformation energy is approximately 3.3 eV for La_2O_3, calculated as the energy difference of this oxide in the space groups *P3m*1 and *Pm*3*m* with a perovskite lattice constant of 3.97 Å. This difference is approximately 4.1 eV for Y_2O_3, calculated as the change from space group *Ia*3 to *Pm*3*m* with a lattice constant of 3.88 Å. Additionally, the interchange between A' and d-block metal atoms implies breaking and creation of bonds, so the swapping energy can be estimated as the difference in the d-band centers ε_d of these atoms. This turns Equation (4) into Equation (5)

$$\Delta G^{\text{form}} = \gamma_{A'_2O_3} + (\varepsilon_{d,A'} - \varepsilon_{d,M}) \quad (5)$$

where $\gamma_{A'_2O_3}$ is a constant that collects the formation energy of the sesquioxide and its deformation and is around -13.6 eV for La_2O_3 and -13.7 eV for Y_2O_3. This constant can be regarded as an intrinsic stability conferred on $A'MO_3$ by its A′ component. As a result, the differences in energies among these perovskites can be attributed to the relative ease of swapping atoms, whereby Ti is the easiest and Cu the hardest along the 3d metal series.

Furthermore, our model is also in agreement with the works by Gelatt et al.[17] devoted to the theory of bonding between transition metals and nontransition elements, and uses the d-band centers of transition metals as key descriptors for understanding the properties of their compounds as in the model by Hammer and Norskov[18] developed for adsorption energies.

In conclusion, DFT gives sufficient atomic-scale insight into perovskites to study their formation energies, both qualitatively and quantitatively, except for a constant shift, and important trends are found. The analysis shown here could be extended to perovskites with 4d and 5d constituents, to perovskites containing alkaline earth elements, and to $ScMO_3$. The combination of the energetics of several reactions and their variations with pH and applied potential can give rise to Pourbaix diagrams for perovskites, which are not yet available in the literature. This and other stability considerations are of paramount importance in any application, especially if perovskites are to be used in alkaline or proton-exchange membrane fuel cells.

Methods

The DFT calculations were performed with the plane wave code DACAPO,[9] using the RPBE exchange-correlation functional, a converged plane wave cutoff of 400 eV and a density cutoff of 500 eV. DACAPO uses ultrasoft pseudopotentials to represent the ion-electron interaction. Atomic relaxations were done with the quasi-Newton minimization scheme until a maximum force below 0.05 eV Å^{-1} between atoms was reached. Besides, we optimized the lattice vectors by minimizing the strain on $2\times2\times2$ supercells in all periodically repeated directions. The Brillouin zone of all systems was sampled with Monkhorst–Pack grids, guaranteeing in all cases that the product of the supercell dimensions and the k-points was at least 25 Å in all directions. The self-consistent RPBE density was determined by iterative diagonalization of the Kohn–Sham Hamiltonian at $k_B T = 0.1$ eV, using Pulay mixing of densities, and all total energies were extrapolated to $k_B T = 0$ eV. Spin-polarized calculations were carried out when needed. See the Supporting Information for further details.

Received: April 19, 2010
Revised: July 15, 2010
Published online: September 10, 2010

Keywords: density functional calculations · heats of formation · perovskites · thermochemistry

[1] G. L. Messing, S. Trolier-McKinstry, E. M. Sabolsky, C. Duran, S. Kwon, B. Brahmaroutu, P. Park, H. Yilmaz, P. W. Rehrig, K. B. Eitel, E. Suvaci, M. Seabaugh, K. S. Oh, *Crit. Rev. Solid State Mater. Sci.* **2004**, *29*, 45.
[2] C. H. Ahn, K. M. Rabe, J. M. Triscone, *Science* **2004**, *303*, 488.
[3] a) S. W. Cheong, M. Mostovoy, *Nat. Mater.* **2007**, *6*, 13; b) J. M. DeTeresa, M. R. Ibarra, P. A. Algarabel, C. Ritter, C. Marquina, J. Blasco, J. Garcia, A. delMoral, Z. Arnold, *Nature* **1997**, *386*, 256.
[4] J. R. Mawdsley, T. R. Krause, *Appl. Catal. A* **2008**, *334*, 311.
[5] T. Nitadori, T. Ichiki, M. Misono, *Bull. Chem. Soc. Jpn.* **1988**, *61*, 621.
[6] a) Y. H. Huang, R. I. Dass, Z. L. Xing, J. B. Goodenough, *Science* **2006**, *312*, 254; b) D. Thiele, A. Zuttel, *J. Power Sources* **2008**, *183*, 590.
[7] a) J. K. Nørskov, T. Bligaard, J. Rossmeisl, C. H. Christensen, *Nat. Chem.* **2009**, *1*, 37; b) J. Greeley, I. E. L. Stephens, A. S. Bondarenko, T. P. Johansson, H. A. Hansen, T. F. Jaramillo, J. Rossmeisl, I. Chorkendorff, J. K. Norskov, *Nat. Chem.* **2009**, *1*, 552; c) F. Studt, F. Abild-Pedersen, T. Bligaard, R. Z. Sorensen, C. H. Christensen, J. K. Norskov, *Angew. Chem.* **2008**, *120*, 9439; *Angew. Chem. Int. Ed.* **2008**, *47*, 9299.
[8] a) G. Pacchioni, *J. Chem. Phys.* **2008**, *128*, 182505; b) M. van Schilfgaarde, T. Kotani, S. Faleev, *Phys. Rev. Lett.* **2006**, *96*, 226402; c) L. Wang, T. Maxisch, G. Ceder, *Phys. Rev. B* **2006**, *73*, 195107.
[9] B. Hammer, L. B. Hansen, J. K. Norskov, *Phys. Rev. B* **1999**, *59*, 7413.
[10] J. I. Martínez, H. A. Hansen, J. Rossmeisl, J. K. Norskov, *Phys. Rev. B* **2009**, *79*, 045120.
[11] S. Kurth, J. P. Perdew, P. Blaha, *Int. J. Quantum Chem.* **1999**, *75*, 889.
[12] E. M. Fernández, P. G. Moses, A. Toftelund, H. A. Hansen, J. I. Martinez, F. Abild-Pedersen, J. Kleis, B. Hinnemann, J. Rossmeisl, T. Bligaard, J. K. Norskov, *Angew. Chem.* **2008**, *120*, 4761; *Angew. Chem. Int. Ed.* **2008**, *47*, 4683.
[13] R. Pankajavalli, O. M. Sreedharan, *Mater. Lett.* **1995**, *24*, 247.
[14] a) J. H. Cheng, A. Navrotsky, X. D. Zhou, H. U. Anderson, *J. Mater. Res.* **2005**, *20*, 191; b) H. Yokokawa, *Annu. Rev. Mater. Res.* **2003**, *33*, 581.
[15] A. N. Grundy, B. Hallstedt, L. J. Gauckler, *J. Phase Equilib.* **2001**, *22*, 105.
[16] M. Binnewies, E. Milke, *Thermochemical Data of Elements and Compounds*, 2nd ed., Wiley-VCH, Weinheim, **2002**.
[17] C. D. Gelatt, A. R. Williams, V. L. Moruzzi, *Phys. Rev. B* **1983**, *27*, 2005.
[18] B. Hammer, J. K. Nørskov in *Advances in Catalysis*, *Vol. 45* (Eds.: C. G. Bruce, K. Helmut), Academic Press, New York, **2000**, p. 71.

